

Nutrients in Amazonian Black Earth from Caxiuanã Region

Vanda P. Lemos,*^a Antônio R. de Oliveira Meireles,^a Kelly das Graças Fernandes,^a
Milena C. de Moraes,^a Marcondes L. da Costa,^b Any K. Terra Silva^b and Dirse C. Kern^c

^aInstituto de Ciências Exatas e Naturais and ^bInstituto de Geociências,
Universidade Federal do Pará, 66075-110 Belém-PA, Brazil

^cMuseu Paraense Emilio Goeldi, Belém-PA, Brazil

Padrões de dispersão de nutrientes em terra preta Amazônica (TPA) podem dar informações sobre atividades antrópicas dos habitantes da Amazônia. Estudos sobre pH, fósforo disponível (P), matéria orgânica (MO) e os cátions trocáveis, Ca²⁺ e Mg²⁺, foram realizados em amostras de solos dos horizontes A₁ e A₂ ao longo de uma área com TPA (norte-sul e leste-oeste) em um sítio arqueológico denominado Ilha de Terra, na Unidade de Conservação Floresta Nacional de Caxiuanã, Município de Melgaço, Brasil. Os resultados indicaram que a MO e o Ca são os que apresentam maior dispersão. Correlações mais elevadas foram encontradas entre OM-Ca-Mg às proximidades da área central e levam a inferir que a dispersão geoquímica de MO, Ca, Mg e P em sítios arqueológicos com TPA está relacionada com atividades humanas progressas.

Dispersion of nutrients in Amazonian black earth (ABE) can provide information on human activities of the inhabitants of the Amazon region. Studies on the pH, available phosphorus (P), organic matter (OM) and the exchangeable cations Ca²⁺ and Mg²⁺ were performed on soil samples from horizons A₁ and A₂ over an area with TPA (north-south and east-west) at a site called Ilha de Terra, located in the Conservation Unit Caxiuanã National Forest, Melgaço County, Brazil. The results indicated that the OM and Ca²⁺ are the ones with greater dispersion. Higher correlations were found between OM-Ca-Mg to near the central area. This leads to the inference that the dispersion geochemistry of MO, Ca, Mg and P in archaeological sites with TPA is related to past human activities.

Keywords: nutrients, Caxiuanã, soils, Amazonian black earth

Introduction

Chemical, mineralogical and micromorphological analysis can be used to interpret human activities from material remains in soils. The abandonment of human activities in settlements does not affect chemical residue remains in soils. The potential validity of the chemical analysis of soil to interpret archaeological finds lies in its ability to predict significant features based on (i) the chemical signatures of total concentrations of multi-elements such as Ba, Ca, P, Zn, Cu and Pb in soils;¹ (ii) the chemical signatures of floor samples in the Maya region;^{2,3} (iii) the available nutrients in soils from the Brazilian Amazon basin,⁴⁻⁸ known by designations such

as black earth, Indian black earth, anthropogenic black earth, archaeological black earth, Amazonian black earth (ABE)^{9,10} or Amazonian dark earths.^{11,12} The area in which ABE occurs is characterized by well-drained soil, running water and located in a particular geographical setting from which the surrounding areas can be clearly observed.⁹

ABE is a soil that can be distinguished from other soils from the Brazilian Amazon because of its high content of Ca, Mg, Zn, Mn, P and C due to the incorporation of bones and organic matter (OM). The high level of organic matter in ABE is attributed to the time of human occupation of the site.¹⁰⁻¹³ According to the soil classification system, ABE sites can be found on several soil classes, such as Oxisols, Ultisols, Inceptisols, Latossolos, Argissolos, Cambissolos, Plintossolos, Espodossolos, Fimic Anthrosols and others.¹⁴

*e-mail: vplemos@ufpa.br

In Latossolos, the organic component is derived from the natural vegetal covering, whereas in ABE the organic component is principally derived from the debris of human occupation. These highly fertile micro-ecosystems formed in the past seem not to exhaust their chemical content in conditions of tropical forest.⁶ The association between soil nutrient level and availability is dependent on the extraction used to determine the nutrient level, soil water regime, physical and chemical soil characteristics controlling nutrient movement and the ability of the plant or plants in question to use the nutrient when it reaches the surface. Nutrient bioavailability is a function of the release of nutrients from their inorganic or organic solid phases, followed by their movement through the soil solution to the roots or fungi, with an ensuing uptake in plant available form.⁷

In the field, ABE soils are identified by unusual features for Amazonian upland soils, such as top soils with dark matrix colors (dark brown to black), the presence of lithic artifacts and pyrogenic carbon.^{9,15} The occurrence of ceramics and black carbon indicates that the genesis of these soils is strongly linked to anthropogenic processes.^{12,16} Several terms are used synonymous with black carbon, such as charcoal, soot, elemental carbon or pyrogenic carbon. Black carbon has been proposed to be an important sink in the global carbon cycle.¹⁵⁻¹⁸ Information on the chemical properties and biological stability of black carbon in soil is limited and more research is needed in this area.

The most accepted theory on the origin of ABE is the anthropogenic evidence demonstrated through the activities of prehistoric humans. The observations of Neves *et al.*¹⁹ indicate that the social practices in settlements with ABE are still not fully understood and that ABE formation was a faster process than previously thought. The increase in population according to the weather could provide an explanation on the formation of ABE but this has not been indicated in sites with multiple occupations. Further research might explain the abandoned settlements in the central Amazon.

Chemical and mineralogical studies on ABE can evaluate the anthropogenic impact on the original soils. An evaluation of the dispersion of nutrients in an area with ABE has been made in this paper. The selected ABE site is called Iha de Terra, located in the area of research called Estação Científica Ferreira Penna (ECFPn), within the National Forest of Caxiuanã (NF-Caxiuanã), belonging to the cities of Portel and Melgaço-Pará in the Amazon region.²⁰

Study area

The national forest of Caxiuanã (NF-Caxiuanã) is located on the west side of the Bay of Caxiuanã downstream

of the Anapu River and the bank of the Xingu River, and includes the cities of Portel and Melgaço in the lower Amazon. NF-Caxiuanã is administered by the Brazilian Institute for Environmental Monitoring (IBAMA) and is protected by the National System of Conservation of Nature from the federal government. The ECFPn built inside the reserve and belonging to the Museu Paraense Emílio Goeldi (MPEG) supports multidisciplinary research on natural sciences. Access to the area is in two steps: the first through the waterway between the cities of Belém and Breves (Ilha do Marajó), lasting for 12 h; the second stage is also a waterway. The journey in this step is made by boat to the ECFPn and passes Hole Breves, the Bay of Melgaço, Anapu river basin toward the source of the river (duration of 9 h), Bay of Caxiuanã, Curuá River until reaching the Trapiche-ECFPn. The area of ECFPn (33,000 hectares) is located north of NF-Caxiuanã and is surrounded by a dense forest area, which ensures optimal conditions for its conservation. Around the edges of the Bay of Caxiuanã, 27 archaeological sites with ABE were discovered. The archaeological site Ilha de Terra is located near the Hole Camuim. Ancient inhabitants of the cities of Portel and Melgaço were the Indians Arucará and Aricuru (also called Guaricuru, Uaricuri or Ingaibas), respectively. Currently, some families are found near the rivers but they do not cause damage to the environment because they preserve the habits of prehistoric man.²¹

Experimental

Soil sampling

The ABE area was delimited from the yellow Latossolos surrounding (YLS). East-west and north-south base lines were traced by auxiliary lines with 10 m spacing for sampling. The sampling was carried out along the ABE area (Figure 1), between two soil profiles (YLS profile and ABE profile), following the methods of Lemos and Santos.²¹ The horizons of the soils were classified according to the methods of the Brazilian System of Soil Classification and color samples were determined according to Munsell collors.²³

Soil analysis

Samples (fractions < 2 mm) of air-dried soil were used in the particle size distribution of the bulk soil, morphological, mineralogical and chemical analysis. Particle size distribution was determined using the sieve/pipette method after ultrasonic dispersion in NaOH 0.01 mol L⁻¹. Morphologies and surface textures of black

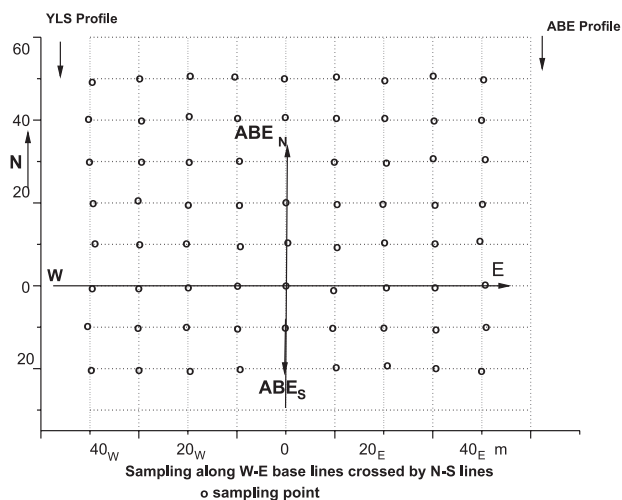


Figure 1. Sampling in ABE area from Ilha de Terra. The ABE area was delimited from the yellow Latossolos surrounding (YLS). East-west and north-south base lines were traced by auxiliary lines with 10 m spacing for sampling.

carbon were examined by scanning electron microscopy (SEM), from thin layers of samples sputtered with Pt to enhance the surface conductivity. SEM analysis was performed under conditions of images obtained by electron backscattering at 20 kV, with a distance of work of 14 mm. Mineralogical analysis was carried out by X-ray diffraction (XRD) using a Philips X-ray diffractometer (PW-1050) with monochromatic Cu-K α radiation. The following chemical analysis were carried out according to the soil survey laboratory methods manual from USDA:²⁴ potentiometric measures of pH (in H₂O and KCl), concentrations for available P, exchangeable Ca²⁺ and Mg²⁺ and the total concentrations for organic C, Si, Al and Fe. Suitable extractors were used in the analysis of available P and exchangeable cations ions to replace or promote the selective dissolution of ions on the surface of minerals and organic substances. Exchangeable Ca²⁺ and Mg²⁺ were extractable with the KCl solution (1 mol L⁻¹) and the available P with the extractor Mehlich-1 (HCl 0.05 mol L⁻¹ plus H₂SO₄ 0.0125 mol L⁻¹). Concentrations of exchangeable Ca²⁺ and Mg²⁺ were measured by atomic absorption spectrometry and the available P by spectrophotometry ($\lambda = 860$ nm) as a blue heterocompound from the reduction of heteropolyacid molybdophosphoric.²⁵

The measurement total organic carbon (TOC) can help the indirect analysis of OM formed during the decay of plant and microbial residues, either by selective preservation and the transformation of constituents resistant to biodegradation and aliphatic polymers, or by the condensation of low-molecular-weight degradation products such as phenols, phenolic acids and amino

acids.^{26,27} TOC was determined by Walkley-Black modified acid-dichromate digestion and FeSO₄ titration. TOC values were multiplied by the Van Bemmelen factor of 1.724 to calculate OM. Black carbon is not determined by the Walkley-Black method, but its presence was investigated by macroscopic observations and SEM analysis.

Total concentrations for Si, Al and Fe were determined using the alkaline fusion method after the dissolution of the sample melted in HCl solution, evaporation of the acid solution, treatment of the residue from this evaporation with concentrated HCl to precipitate silica, filtration (solution A) and separation of the precipitate, treatment of the precipitate with a mixture of H₂SO₄:HF (1:200), calcination and weighing the final residue. Solution A was used to measure the concentrations of Al and Fe by AAS-flame.

The significance of the variability of the chemical elements and correlation coefficients for these elements from the ABE area was evaluated by analysis of variance of values (F) and correlation matrix, respectively. The variance values were determined for the CCABE areas north, south, central, north-south and west-east, indicated in this study as ABE_N, ABE_S, ABE_{central}, ABE_{N-S} and ABE_{W-E}, respectively.

Results and Discussion

The soil horizons

The following horizons were observed in the ABE profile: A₁ and A₂ black (0-7 cm and 7-14 cm, respectively), A₃ dark brown (14-29 cm), AB dark grayish brown (29-57 cm), BA brown (57-89 cm) and B₁, B₂ and B₃ brownish yellow (89-110, 110-135 and 135-161 cm, respectively). The YLS profile presents the following: A₁ horizon dark grayish brown (0-8 cm), AB and BA horizons brownish yellow (8-20 and 20-59 cm, respectively) and B₁, B₂ and B₃ horizons dark yellowish Brown (59-100, 100-162 and 162-180 cm, respectively).

Physical and chemical properties

The high OM, available P, exchangeable Ca²⁺ and Mg²⁺ content (Tables 1-3) and frequent occurrence of BC are diagnostic attributes of anthropogenic soils. BC occurs in the forms of irregular fragments micrometer to millimeter and fibrous texture (Figure 2). Studies on BC in soils from other sites have shown great variability in sizes, shapes and chemical composition of particles of BC. It has also been found numerous particles of BC in the medium density fraction indicating organ-mineral complexes and the distribution of BC across aggregate fractions in close contact with minerals.²⁸⁻³¹

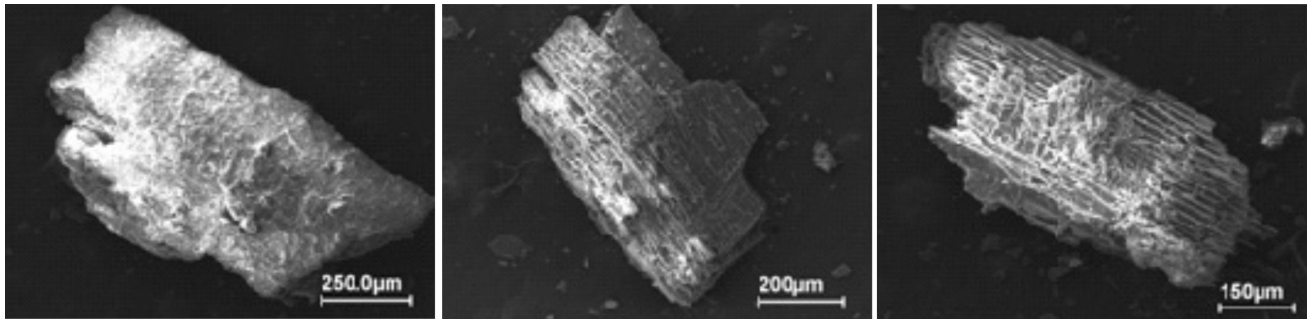


Figure 2. Fragments of black carbon with micrometer dimensions, irregular shapes and fibrous texture from A₁ horizon-ABE soil profile.

The physical and chemical properties in the soil profiles from ABE and YLS shows that the main differences between the two soil profiles are observed in the upper horizons of the soil profiles (Table 1 and Figure 3). Particle size distribution indicates a predominance of coarse sand fraction on the other fractions in soil profiles ABE and YLS, and this allows the identification of the types of textures. In the ABE profile, the texture is sandy in A₁ to BA and sandy-clay in B, whereas in the YLS profile the. Data from X-ray diffraction show that the horizons A₁ of soil profiles ABE and YLS have quartz as main mineral. Reflections of kaolinite were identified only in the soil profile YLS (Figure 3). Anatase, goethite and or hematite were not identified because they must occur at low frequencies, given the low concentrations of Ti and Fe obtained in these soils.

From the total concentrations of SiO₂, Al₂O₃, Fe₂O₃ and OM (Table 1) it was estimated the concentrations of the minerals and organic matter in both soil profiles. It was verified that kaolinite and quartz are the predominant

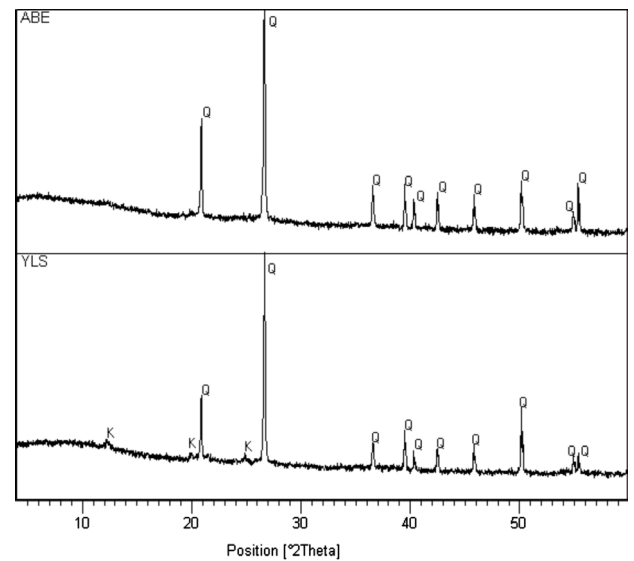


Figure 3. XRD pattern for the archaeological black earth (ABE) and yellow Latossolos surrounding (YLS) from Ilha de Terra-Caxiuanã. Symbols: Q = quartz, K = kaolinite.

Table 1. Physical and chemical properties of the ABE soil profile and YLS soil profile. Concentrations of organic matter (OM), Ca²⁺, Mg²⁺, available P in mg kg⁻¹; coarse sand, fine sand, silt, clay, OM, SiO₂, Al₂O₃ and Fe₂O₃ in g kg⁻¹

Horizons	C.S ^b	F.S ^c	Silt	Clay	pH (H ₂ O)	pH (KCl)	OM	SiO ₂	Al ₂ O ₃	Fe ₂ O ₃	P	Ca ²⁺	Mg ²⁺
ABE-A ₁	560	190	190	60	4.5	3.83	171	783.6	73.8	18.5	135	1708	158
ABE-A ₂	560	160	200	80	4.9	3.89	126	737.1	75.7	19.6	96	984	127
ABE-A ₃	530	170	210	90	5.11	4.18	77	718.5	79.1	22.1	127	648	67
ABE-AB	520	170	220	90	5.26	4.38	27	704.3	98.6	29.8	99	520	31
ABE-BA	500	150	230	120	5.26	4.36	25	698.4	98.8	34.6	69	480	24
ABE-B ₁	470	140	230	160	5.36	4.61	20	685.7	111.6	38.1	79	220	22
ABE-B ₂	440	110	240	210	5.59	4.79	12	678.8	142.5	40.3	100	232	22
ABE-B ₃	420	110	240	230	5.87	4.91	8	665.0	150.2	50.8	88	84	19
YLS-A ₁	470	200	150	180	4.06	3.60	2	705.0	93.4	30.5	18	20	7.2
YLS-AB	440	180	170	210	4.13	3.73	1.8	681.3	124.6	45.8	17	20	7.2
YLS-BA	410	170	180	240	4.22	4.00	1.6	659.2	152.8	51.0	13	20	4.8
YLS-B ₁	390	170	180	260	4.24	4.02	1.2	651.3	162.9	53.6	48	16	4.8
YLS-B ₂	390	130	190	290	4.46	4.05	1.2	636.4	178.1	67.2	48	12	4.8
YLS-B ₃	370	110	220	300	4.58	4.05	0.8	632.0	197.2	79.3	51	12	4.8

^aP-Mehlich-1; ^bCoarse sand; ^cFine sand.

minerals in both soil profiles. The concentrations of kaolinite increases with depth in both profiles, being more pronounced in the YLS profile. Goethite has a lower concentration than that of kaolinite and quartz in all profiles. The horizon A of the ABE profile has a higher concentration in SiO_2 and OM as well as lower concentrations of Al_2O_3 and Fe_2O_3 compared with those of the A horizon from the YLS profile. In both soil profiles, there is an increase of the $\text{SiO}_2/\text{Al}_2\text{O}_3$ ratio toward the surface, with the increase in the ABE profile greater than in the YLS profile. The increase in the $\text{SiO}_2/\text{Al}_2\text{O}_3$ ratio indicates that the soils have lost Al_2O_3 , resulting in an accumulation of quartz.

Figures 4 and 5 show the variability of the concentrations of OM compared with other chemical properties (available P and exchangeable Ca^{2+} and Mg^{2+}) along the soils profiles. In the ABE soil profile are observed increase in the concentrations of Ca with those of OM; small variability in the concentrations of Mg and P. In the YLS soil profile was observed higher concentrations of OM in the horizons AB, BA and B_1 and of P in the horizons B_1 to B_3 ; slight increase in Ca concentrations towards the surface. The greater pH in the A horizon from the ABE profile and ABE area compared with those of the YLS (Table 1) is the result of higher base cation saturation of the cation exchange. This feature was observed in each site and might be the result of base cation inputs during site habitation.²¹ pH has a further importance because it can determine a variety of nutrient transformation and toxicity relationships in soils.⁷

These data show that the values for pH and OM, available P and exchangeable Ca^{2+} and Mg^{2+} concentrations in ABE are compatible with those obtained from other sites in the Caxiuanã region.²¹ It was estimated from the difference between pH (H_2O) and pH (KCl) that the ABE and YLS soils from Ilha de Terra presents ΔpH between -1.08 to -1.09 and -0.52 to -1.31 , respectively. Surface charge is usually determined by the difference between pH_{ZPC} , the point of zero charge, and the actual soil pH, such that if $\text{pH}_{\text{ZPC}} - \text{pH}$ is negative then the surface charge is negative.³²⁻³⁵

Considering the mineralogical and chemical properties of the soils from Ilha de Terra, it has been suggested that they have a negative charge and that OM is mainly responsible for this development. Quartz, anatase, goethite and hematite contain a negligible charge.³⁶ The tetrahedral sheet of kaolinite carries a small permanent negative charge because of isomorphous substitution of Si^{4+} by Al^{3+} , leaving a single negative charge for each substitution. Both the octahedral sheet and the crystal edges have a dependent variable charge caused by the protonation and deprotonation of surface hydroxyl (SOH) groups. Thus, tetrahedral sites of clay become permanently negatively

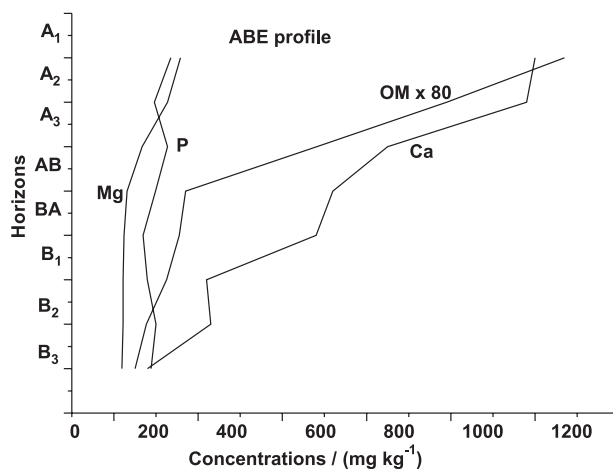


Figure 4. Concentrations of organic matter (OM) compared with other chemical properties along the horizons of the ABE soil profile.

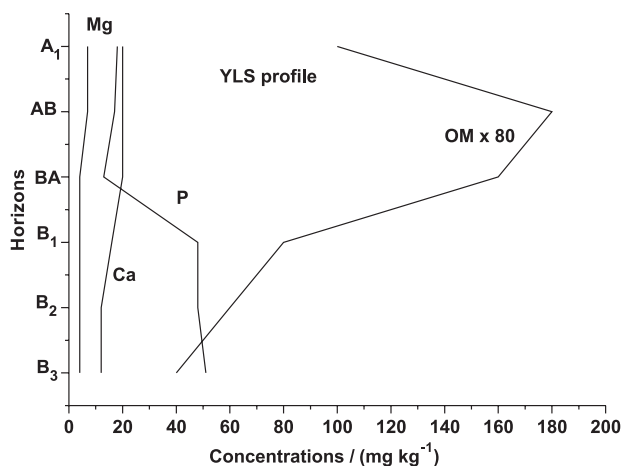


Figure 5. Concentrations of organic matter (OM) compared with other chemical properties along the horizons of the YLS soil profile.

charged and allow the electrostatic interaction with positively charged ions. However, this permanent charge is a minor component in kaolinite-type clays. The layer edges where exposed OH groups will exhibit acid-base behavior are primarily responsible for the interaction of kaolinite with environmental metal ions. Crystalline oxide of iron (hematite) is widely distributed in soils and has a surface that is normally hydrated so it can participate in adsorption reactions similar to those of hydrous. Soil pH_{ZPC} can be altered by adding OM.³⁶ Therefore, the appropriate manipulation of the soils can lead to an increase in surface negative charge.³²

Geochemical dispersion

The release and retention of OM, Ca, Mg and P in soils with ABE is a dynamic process that is dependent on the pH and mineralogy of the soils and chemistry composition of the soils solution. The variability of these properties in the area

ABE is reflected through the concentrations (Tables 2 and 3) and variances (Table 4). OM and Ca are the components of soils that have a higher dispersion in all directions from the ABE area (north, south, central, north-south and east-west). Values of variance indicate that the dispersion of P and Mg are also important but are much lower than those obtained for OM and Ca. The highest concentrations of OM were observed in the southwest and northwest and the lowest in the northeast and southeast of the ABE area. In some places in ABE area, a sharp decrease in the concentrations of Ca

and OM were observed, for example in the central area, north-south and east-west (Figures 6 and 7). It is possible that the spaces in the area with the lowest concentrations of OM and Ca have been used by ancient inhabitants as preferential sites for religious ceremonies, the spaces with highest concentrations of OM and Ca have been used as preferential sites for food preparation and the accumulation of waste and a small area with high concentrations of Ca, Mg and P has been reserved as a cemetery. Many Indian villages have a cleared space in the central area that is kept clean for

Table 2. Chemical properties from soils with archaeological Black earth along N-S area

(N-S)	Ph		OM / (mg kg ⁻¹ ×10 ³)		Ca / (mg kg ⁻¹)		Mg / (mg kg ⁻¹)		P / (mg kg ⁻¹)	
	A ₁	A ₂	A ₁	A ₂	A ₁	A ₂	A ₁	A ₂	A ₁	A ₂
(m)	A ₁	A ₂	A ₁	A ₂	A ₁	A ₂	A ₁	A ₂	A ₁	A ₂
50	4.44	4.72	86	70	300	200	156	120	250	220
40	4.16	4.38	76	76	540	440	126	120	274	422
35	4.47	4.61	92	76	710	600	102	108	296	392
20	4.52	4.66	83	62	800	540	132	120	333	391
10	4.21	4.44	73	71	610	460	110	96	378	447
0	4.02	4.5	86	80	490	440	110	132	356	435
10	4.03	4.04	83	94	600	600	84	50	410	460
20	4.26	4.45	145	123	580	580	140	70	350	475

Table 3. Chemical properties from soils with archaeological Black earth along W-E area

W-E	pH		OM / (mg kg ⁻¹ ×10 ³)		Ca / (mg kg ⁻¹)		Mg / (mg kg ⁻¹)		P / (mg kg ⁻¹)	
	A ₁	A ₂	A ₁	A ₂	A ₁	A ₂	A ₁	A ₂	A ₁	A ₂
(m)	A ₁	A ₂	A ₁	A ₂	A ₁	A ₂	A ₁	A ₂	A ₁	A ₂
40	4.83	4.70	108.0	96.80	1036	620	129	116	541	418
30	4.54	4.55	142.4	108.6	545	420	99	106	521	390
20	4.48	4.51	104.0	107.2	600	389	147	120	533	467
10	4.41	4.42	90.00	87.00	503	340	141	113	484	419
00	4.47	4.30	78.00	70.64	497	356	93	92	525	348
10	4.36	4.41	65.60	58.84	411	289	113	78	423	365
20	4.16	4.47	50.80	75.60	332	230	110	80	380	228
30	4.26	4.41	74.48	69.60	255	320	130	106	358	284
40	4.10	4.28	94.00	93.30	95	274	102	93	367	236

Table 4. Variance of chemical properties from ABE areas north, south, central, north-south and west-east, as ABE_N, ABE_S, ABE_{CENTRAL}, ABE_{N-S} and ABE_{W-E}, respectively

ABE Area	pH		OM		Ca		Mg		P	
	A ₁	A ₂	A ₁	A ₂	A ₁	A ₂	A ₁	A ₂	A ₁	A ₂
ABE _N	128	99	1×10 ⁹	381	40254	22690	654	113	2629	1604
ABE _S	32	7	969	752	2128	25400	12357	10978	9398	12424
ABE _{CENTRAL}	13	15	1429	987	156592	7441	1790	2694	10312	26998
ABE _{N-S}	18	20	5×10 ⁸	9×10 ⁸	22098	18914	528	750	2925	6651
ABE _{W-E}	22	20	8×10 ⁸	3×10 ⁸	69232	12924	371	236	5903	7142

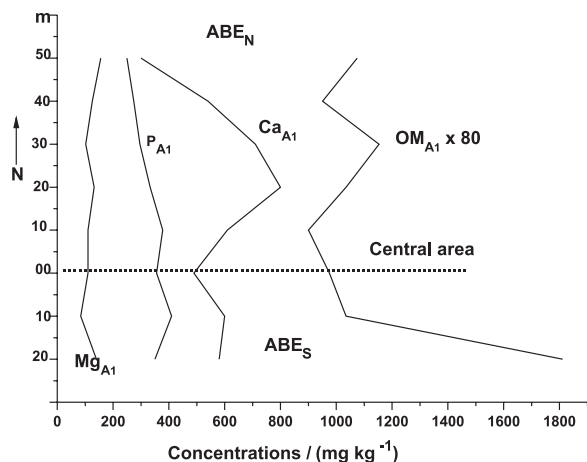


Figure 6. Concentrations of the available P, exchangeable Ca^{2+} and Mg^{2+} and OM (multiplied by 80) in north to south of the area $\{(ABE)_{N,S}\}$.

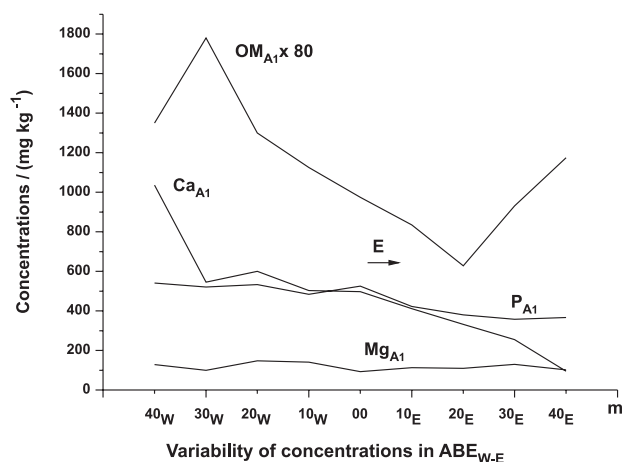


Figure 7. Concentrations of the available P, exchangeable Ca^{2+} and Mg^{2+} and OM (multiplied by 80) in west-east area $\{(ABE)_{W,E}\}$.

Table 5. Correlation matrix of chemical properties from soils with archaeological Black earth from ABE area N-S

	$(ABE)_N: 50_N$				$(ABE)_N: 40_N$				$(ABE)_N: 30_N$				$(ABE)_N: 20_N$			
	OM	P	Ca	Mg	OM	P	Ca	Mg	OM	P	Ca	Mg	OM	P	Ca	Mg
OM	1				1				1				1			
P	0.2	1			0.3	1			0.01	1			0.01	1		
Ca	0.3	0.41	1		0.6	0.5	1		0.01	0.5	1		0.6	0.3	1	
Mg	0.3	0.1	0.2	1	0.3	0.3	0.4	1	0.01	0.2	0.6	1	0.5	0.2	0.5	1
	$(ABE)_N: 10_N$				ABN: central				$(ABE)_S: 10_S$				$(ABE)_S: 20_S$			
	OM	P	Ca	Mg	OM	P	Ca	Mg	OM	P	Ca	Mg	OM	P	Ca	Mg
OM	1				1				1				1			
P	0.1	1			0.1	1			0.4	1			0.4	1		
Ca	0.5	0.4	1		0.6	0.1	1		0.8	0.6	1		0.3	0.2		
Mg	0.6	0.2	0.8	1	0.2	0.3	0.5	1	0.3	0.01	0.5	1	0.2	0.01	0.01	1

ceremonial events whereas rubbish is commonly deposited at the perimeter of the ancient settlement.⁹

Geochemical correlation

The similarities and differences among the distribution patterns of OM, Ca, P and Mg can be estimated through the correlation coefficients shown in Table 5. The highest correlation coefficients were obtained between pairs OM-Ca and Ca-Mg. However, it has been shown that the interpretation of element concentrations patterns in archaeological soils is problematic because of the complexity of site use history and the effects of post-depositional soil processes. Many human activities can add element loadings to cultivated soils. However, a host of natural and anthropogenic factors can affect total soil concentrations. Background variation linked to differences in soils can result in patterns of element concentration unconnected to the archaeology.¹

Conclusions

The physicochemical properties of the soil profiles ABE and YLS suggested the soils of these profiles belonged to the same class of soil before human occupation. The activities performed by the ancient inhabitants of the region caused changes in the upper horizons of that soil class. This hypothesis is shown in this study through the following data: changing of the yellow color of Latossolos to black, dark brown and light brown because of the presence of black carbon and the accumulation of OM originated from animal and vegetable waste; changing of the soil texture from sandy-clay to sandy because of human settlement, which decreased the concentrations of Al and increased those of Si due to the formation of quartz; lower concentrations of OM, exchangeable Ca^{2+} and Mg^{2+} and available P in the spaces near the central area suggesting that these spaces were reserved for religious ceremonies or other events.

Acknowledgments

This study was made possible by sampling support of the Museu Paraense Emilio Goeldi and financial support of the Conselho Nacional de Desenvolvimento Científico e Tecnológico (CNPq).

References

1. Wilson, C. A.; Davidson, D. A.; Cresser, M. S.; *J. Archaeol. Sci.* **2008**, *35*, 412.
2. Parnell, J. J.; Terry, R. E.; *J. Archaeol. Sci.* **2002**, *29*, 379.
3. Fernandez, F. G.; Terry, R. E.; Inomate, T.; Eberl, M.; *Geoarchaeology* **2002**, *17*, 487.
4. Lima, H. N.; Schaefer, C. E. R.; Melo, J. W. V.; Gilkes, R. J.; Ker, J. C.; *Geoderma* **2002**, *110*, 1.
5. Cunha, T. J. F.; Madari, B. E.; Canellas, L. P.; Ribeiro, L. P.; Benites, V. M.; Santos, G. A.; *R. Bras. Ci. Solo* **2009**, *35*, 85.
6. Lehmann, J.; Kern, D.; German, L.; Mccann, J.; Martins, G. C.; Moreira, A. In *Amazonian Dark Earths: Origin, Properties, Management*; Lehmann, J.; Kern, D. C.; Glaser, B.; Woods, W. I., eds.; Kluwer Academic Publishers: Boston-London, 2003, ch. 6.
7. Falcão, N. P. S.; Comerford, N.; Lehmann, J. In *Amazonian Dark Earths: Origin, Properties, Management*; Lehmann, J.; Kern, D. C.; Glaser, B.; Woods, W. I., eds.; Kluwer Academic Publishers: Boston-London, 2003, ch. 14.
8. Novotny, E. H.; Hayes, M. H. B.; Madari, B. E.; Bonagamba, T. J.; Azevedo, E. R.; Souza, A. A.; Song, G.; Nogueira, C. M.; Mangrich, A. S.; *J. Braz. Chem. Soc.* **2009**, *20*, 1003.
9. Smith, N. J. H.; *Annals of the Association of American Geographers* **1980**, *70*, 553.
10. German, L. A.; *Geoderma* **2003**, *111*, 307.
11. Woods, W. I.; McCann, J. M. *Yearbook Conference of Latin Americanist Geographers*, 1999.
12. Woods, W. I.; McCann, J. M.; Meyer, D. W. *Schoolmaster, F. A. Papers and Proceedings of the Applied Geography Conferences*, 2000.
13. Kern, D. C.; Kämpf, N. R.; *R. Bras. Ci. Solo* **1989**, *13*, 219.
14. Kämpf, N. R.; Woods, W. I.; Sombroek, W.; Kern, D. C.; Cunha, T. J. F. In *Amazonian Dark Earths: Origin, Properties, Management*; Lehmann, J.; Kern, D. C.; Glaser, B.; Woods, W. I., eds.; Kluwer Academic Publishers: Boston-London, ch. 5.
15. Haumaier, L.; Zech, W.; *Org. Geochem.* **1995**, *23*, 191.
16. Glaser, B.; Haumaier, L.; Guggenberger, G.; Zech, W.; *Org. Geochem.* **1998**, *29*, 811.
17. Golchin, A.; Baldock, J. A.; Clarke, P.; Higashi, T.; Oades, J. M.; *Geoderma* **1997**, *76*, 175.
18. Ribeiro, L. G. L.; Carreira, R. S.; Wagener, A. L. R.; *J. Braz. Chem. Soc.* **2008**, *19*, 1277.
19. Neves, E. G.; Petersen, J. B.; Bartone, R. N.; Silva, C. A. In *Amazonian Dark Earths: Origin, Properties, Management*; Lehmann, J.; Kern, D. C.; Glaser, B.; Woods, W. I., eds.; Kluwer Academic Publishers: Boston-London, 2003, ch.3.
20. Kern, D. C.; D'aquino, G.; Rodrigues, T. E.; Frazão, F. J.; Sombroek, W.; Myers, T. P.; Neves, E. G. In *Amazonian Dark Earths: Origin, Properties, Management*; Lehmann, J.; Kern, D. C.; Glaser, B.; Woods, W. I., eds.; Kluwer Academic Publishers: Boston-London, 2003, ch. 4.
21. Costa, M. L.; Kern, D. C.; *J. Geochem. Explor.* **1999**, *66*, 369.
22. Lemos, A.; Santos, P. B.; *Manual de Descrição e Coleta de Solos em Campo*; Sociedade Brasileira de Ciência do Solo: Viçosa, Brasil, 2002.
23. Munsell Colors Company; *Munsell Soil Colors Charts*, Baltimore, 2000.
24. Soil Survey Staff, National Soil Survey Laboratory; *Methods Manual: Soil Survey Investigations Report 42*, version 4.0; United States Department of Agriculture, Natural Resources Conservation Service, National Soil Survey Center, US Govt print Office: Washington, DC, 2004.
25. Shriver, D. F.; Atkins, P. W.; *Química Inorgânica*, Bookman: São Paulo, Brasil, 2008.
26. Stumm, W.; Morgan, J. J.; *Aquatic Chemistry. Chemical Equilibria and Rates in Natural Waters*, John Wiley & Sons: New York, 1996.
27. Schmidt, M. W. I.; Heike, K. H.; Kögel-Knabner, I.; *Org. Geochem.* **2000**, *31*, 727.
28. Glaser, B.; Balashov, E.; Haumaier, L.; Guggenberger, G.; Zech, W.; *Org. Geochem.* **2000**, *31*, 669.
29. Brodowski, S.; Rodionov, A.; Haumaier, L.; Glaser, B.; Amelung, W.; *Org. Geochem.* **2005b** *36*, 1299.
30. Brodowski, S.; John, B.; Flessa, H.; Amelung, W.; *Eur. J. Soil Sci.* **2006**, *59*, 539.
31. Brodowski, S.; Amelung, W.; Haumaier, L.; Zech, W.; *Geoderma* **2007**, *139*, 220.
32. Van Ranst, E.; Shamshuddin, J.; Baert, G.; Dzwowa, P. K.; *Eur. J. Soil Sci.* **1998**, *49*, 243.
33. Gilman, G. P.; *Aust. J. Soil Res.* **1985**, *23*, 643.
34. Gilman, G. P.; Sumpter, E. A.; *Aust. J. Soil Res.* **1986**, *24*, 173.
35. Kaiser, K.; Guggenberger, G.; *Org. Geochem.* **2000**, *31*, 71.
36. Anderson, S. J.; Sposito, G.; *Soil Sci. Soc. Am. J.*; **1991**, *55*, 1569.
37. Kennedy, J.; Billett, M. F.; Duthie, D.; Fraser, A. R.; Harrison, A. F.; *Eur. J. Soil Sci.* **1996**, *47*, 625.

Submitted: April 6, 2010

Published online: January 27, 2011